Journal of Molecular Liquids 393 (2024) 123580

Contents lists available at ScienceDirect

Journal of Molecular Liquids

journal homepage: www.elsevier.com/locate/molliq

Aromatic aldehyde oxidation by hexacyanoferrate(III) catalyzed by Ru(VI) in alkaline medium

C.I. Alcolado [a,b], J. Poblete [c], L. García-Río [d], E. Jiménez [a,b], F.J. Poblete [a,b,*]

[a] Dept. of Physical Chemistry, Faculty of Chemical Science and Technology, University of Castilla-La Mancha (UCLM), Avda. Camilo José Cela 1B, 13071 Ciudad Real, Spain
[b] Research Insitute on Combustion and Atmospheric Pollution (ICCA, Instituto de Investigación en Combustión y Contaminación Atmosférica), UCLM, Camino de Moledores s/n, 13071 Ciudad Real, Spain
[c] Dept. of Inorganic, Organic Chemistry and Biochemistry, Faculty of Chemical Science and Technologies, University of Castilla-La Mancha (UCLM), Avda. Camilo José Cela, 13071 Ciudad Real, Spain
[d] Dept. of Physical Chemistry, Faculty of Chemistry, University of Santiago de Compostela, Avda. Das Ciencias s/n., 15701 Santiago de Compostela, Spain

ARTICLE INFO

Keywords:
Oxidation mechanism
Aromatic aldehydes
Ruthenate ion
Hexacyanoferrate(III)
Alkaline medium

ABSTRACT

In this study, the selective oxidation of aromatic aldehydes has been investigated using Ru(VI) as a catalyst and hexacyanoferrate (III) as a cooxidant in an alkaline medium. The reaction order with respect to the oxidant and the aromatic aldehyde is complex while the reaction order with respect to Ru(VI) is one. The proposed mechanism presents two catalytic cycles for the two active species of the catalyst. In each cycle, Ru(VI) species forms a complex with the anion of hydrated benzaldehyde which decomposes to form benzoic acid. The function of hexacyanoferrate(III) is the regeneration of catalyst species. A quantitative structure–activity relationship was analyzed using the Hammett equation for decomposition complex step. This analysis showed that deactivating groups in *para*- position enhances this process.

1. Introduction

The oxidation of aromatic aldehydes, such as benzaldehyde, in a basic medium, is a reaction of great interest within organic chemistry since their oxidation products, e.g. benzoic acid and its derivatives, are used as precursors in the pharmaceutical and chemical industries. These acids are commonly used as preservatives and/or flavoring agents in food, cosmetics, hygiene, and pharmaceutical products. They are also employed as additives, nucleating agents, intermediates, stabilizers, and/or catalysts in the refrigerant, solvent, photography, plastic, textile, pesticide, paper, and dye industries [1]. Approximately 90 % of commercial benzoic acid is used as an intermediate product for nylon production. Moreover, benzoic acid and its derivatives are found naturally in plant and animal tissues, and they can also be generated in fermented products through microbial metabolism.

At room temperature, benzaldehyde is a colorless liquid with a very distinctive odor that imparts the aroma of bitter almonds, for example. It is poorly soluble in water (3 g/L), leading to low reactivity in this medium. However, it is well known that benzaldehyde derivatives are oxidized to benzoic acid in the presence of oxidants like oxygen [2], hexacyanoferrate (III) [3], or peroxynitrite [4].

In contrast to prior research that has primarily focused on the outer-sphere reduction of hexacyanoferrate(III) by aliphatic and aromatic aldehydes in alkaline conditions [3], our study introduces an innovative perspective by thoroughly investigating this reaction employing a Ru (VI) catalyst in the oxidation process of aromatic aldehydes.

The selective oxidation of organic compounds by transition metal ions, including Ru(III), Ru(IV), and Ru(VI), in the presence of cooxidants like hexacyanoferrate (III), has attracted considerable attention in alkaline media. The presence of Ru(VI) favors the oxidation process since this metal can change its coordination number and oxidation states, preventing the oxidation of certain sensitive bonds through the formation of intermediate complexes [5].

Particularly, the ruthenate anion, $[RuO_4]^{2-}$, a species capable of acting as two electron oxidant in an alkaline medium, is also used as a catalyst with different cooxidants due to its selectivity, making it

* Corresponding author at: Dept. of Physical Chemistry, Faculty of Chemical Science and Technology, University of Castilla-La Mancha (UCLM), Avda. Camilo José Cela 1B, 13071 Ciudad Real, Spain; Research Insitute on Combustion and Atmospheric Pollution (ICCA, Instituto de Investigación en Combustión y Contaminación Atmosférica), UCLM, Camino de Moledores s/n, 13071 Ciudad Real, Spain.
E-mail address: FcoJavier.Poblete@uclm.es (F.J. Poblete).

https://doi.org/10.1016/j.molliq.2023.123580
Received 6 October 2023; Received in revised form 10 November 2023; Accepted 12 November 2023
Available online 23 November 2023

increasingly important and necessary in the oxidation of organic compounds [6,7].

The use of Ru(VI) represents the future of synthetic chemistry perfectly suited to green chemistry. This type of catalysts reduces the formation of residues in addition to having a high selectivity in the reactions involved. On the other hand, ruthenium oxides present a low toxicity level [8,9]. In this way, the production of dangerous compounds is minimized. In addition, some Ru(VI)-catalyzed reactions occur under milder conditions, which reduces energy consumption and their environmental impact [10].

In the present work, a new mechanism that takes in account all aldehydes' equilibria in basic medium, has been proposed in order to justify all the experimental data. This research presents valuable insights into the knowledge of this type of reactions, which opens new possibilities for the development of more efficient and environmentally friendly oxidation methods.

2. Material and methods

2.1. Reagents

All the reagents used were purchased from Sigma-Aldrich with the quality "for analysis", except ruthenate that was synthesized as described below. The selected benzaldehydes were: benzaldehyde (BZH), 4-hydroxybenzaldehyde (*p*-HBZH), 4-methoxybenzaldehyde (*p*-MoxBZH) and 4-nitrobenzaldehyde (*p*-NBZH). The cooxidant used was potassium hexacyanoferrate(III) ($[Fe(CN)_6]^{3-}$), and sodium hydroxide (NaOH) and sodium perchlorate ($NaClO_4$). All the solutions were prepared with double-distilled water.

2.2. Synthesis of Ru (VI) catalyst (sodium ruthenate)

Step 1: Synthesis Ru(VIII) was carried out according to the experimental procedure described by Sandrine Rup et al. [11] $NaIO_4$ and RuO_2 were mixed in water and this solution was stirred for 60 min until complete dissolution. Later CCl_4 was added to the reaction to extract RuO_4. The organic phase presents a bright yellow color due to Ru(VIII) species.

Step 2: Synthesis of ruthenate anion $[RuO_4]^{2-}$; to the previous organic phase, NaOH 1 M was added and the mixture was left in agitation at 25 °C for 20 min to obtain $[RuO_4]^{2-}$ present in the aqueous phase (orange color). This process was repeated three times to improve the ruthenate yield. The aqueous phase with Ru(VI) was left in agitation for 24 h at 25 °C. Subsequently, the absorption spectrum of Ru(VI) was measured by diluting 2 ml of the solution with 1 M NaOH to a final volume of 10 ml. The exact concentration of $[RuO_4]^{2-}$ was calculated from the absorbance at $\lambda = 465$ nm ($\varepsilon = 1820\ mol^{-1}\ cm^{-1}$) [12]. The purity of the solution was confirmed by the absorbance ratio A_{465}/A_{385}. This ratio is the ratio between Ru(VI) and Ru(VII), taking into account that pure ruthenate corresponds to a value of 2.07 [13].

The ruthenate anion $[RuO_4]^{2-}$ is obtained as a product of the reduction of RuO_4 in a basic medium (*reaction (1)*), through the perruthenate species $[RuO_4]^{-}$ via *reaction (2)* [12,14,15].

$$4RuO_4 + 4OH^- \rightarrow 4[RuO_4]^- + 2H_2O + O_2 \quad (1)$$

$$4[RuO_4]^- + 4OH^- \rightarrow 4[RuO_4]^{2-} + 2H_2O + O_2 \quad (2)$$

The alkaline solutions containing $[RuO_4]^{2-}$ are not stable for extended periods due to *reaction (3)*, which produces Ru(VII) and Ru(IV) [7]. Therefore, the control spectrum was conducted daily to monitor the concentration of the ruthenate anion. If the absorbance ratio falls below two, the ruthenate species will be freshly prepared.

$$3[RuO_4]^{2-} + (2+x)H_2O \rightleftharpoons 2[RuO_4]^- + RuO_2{\cdot}xH_2O + 4OH^- \quad (3)$$

2.3. Procedure and measurements

2.3.1. Kinetic study

A spectrophotometric technique was employed to monitor the control chemical species, potassium hexacyanoferrate(III), $[Fe(CN)_6]^{3-}$, by using a Shimadzu UV-160 UV–Vis-NIR Spectrophotometer (Kyoto, Japan). The concentration of $[Fe(CN)_6]^{3-}$ was measured at the absorption maximum wavelength ($\lambda = 420$ nm) using a molar absorptivity of $\xi = (975.52 \pm 0.02)\ M^{-1}\ cm^{-1}$. The temperature of the solution was controlled by an external water circulation system connected to a Selecta Ultraterm S-383 thermostat, with a constant temperature of (25.0 ± 0.5) °C.

The experimental procedure was the following one:

Two solutions (A and B) were prepared and mixed by 50 %. Solution A contains the benzaldehyde derivative and $NaClO_4$, used to control the ionic strength of the solution. Solution B contains hexacyanoferrate(III) and $[RuO_4]^{2-}$ in diluted NaOH and $NaClO_4$. In each kinetic experiment, pH (12.3) was monitored using a pH meter (Crison micropH 2000, Barcelona, Spain). Table 1 shows the concentrations of all species used in the experimental procedure.

All experiments were performed in presence and absence of Ru(VI) and were repeated five times under the same experimental conditions to ensure the reproducibility of the study.

2.4. Kinetic analysis

The experimental data were analyzed using the *initial rate method* which avoids problems as: interferences from reaction products, self-decomposition of reactants, inhibition or autocatalysis effects or the presence of competitive reactions.

To obtain the initial reaction rate (v_0) of each experiment, the method described by Fernández et al. [16]. This method consists of adjusting all the experimental absorbance (A)-time data corresponding to one experiment to a fourth-degree polynomial, $A = a + bt + ct^2 + dt^3 + et^4$. Considering the Lambert-Beer law, the first derivative of this obtained equation yields *b*. The initial rate is then obtained by simply dividing by the extinction coefficient (ε) and the optical pathlength (l = 1 cm) (*Equation (4)*).

$$v_o = -\left(\frac{d\left[[Fe(CN)_6]^{3-}\right]}{dt}\right)_0 = -\left(\frac{b}{\varepsilon l}\right) \quad (4)$$

The experimental values obtained in this kinetic study represent the arithmetic mean of the results from five independent experiments carried out under the same experimental conditions. The associated errors are the standard deviation of the mean.

3. Results

To obtain the experimental rate equation, the influence of substrate concentrations, oxidant, catalyst, and ionic strength has been evaluated. The obtained results are presented in the following sections. The initial rate data used for the kinetic analysis is the difference between the initial reaction rate obtained in the presence of catalyst and that of direct oxidation by $[Fe(CN)_6]^{3-}$ without catalyst. The average contribution of the uncatalyzed reaction was ~15 %. For example, for benzaldehyde (1.00×10^{-3} M) and $[Fe(CN)_6]^{3-}$ (1.20×10^{-3} M), with an ionic strength of 0.5 M, the initial rate of the catalyzed reaction was (2.75 ± 0.03) $\times 10^{-7}$ M/s, while for the reaction without the catalyst, v_0 was

Table 1
Concentrations used in the experimental procedure.

[R-BZH] (M)	$[[Fe(CN)_6]^{3-}]$ (M)	[Ru(VI)] (M)	$[NaClO_4]$ (M)
$(1.00–5.00) \times 10^{-3}$	$(0.60–2.00) \times 10^{-3}$	3.00×10^{-6}	0.5

$(4.24 \pm 0.01) \times 10^{-8}$ M/s, then the initial rate used will be $(2.33 \pm 0.04) \times 10^{-7}$ M/s.

In the following sections, p-hydroxybenzaldehyde (*p*-HBZH) was chosen as example to present the experimental results, the rest of the studied aldehydes are included in the supporting information.

3.1. Influence of substrate concentrations on reaction rate

To analyze this effect, a series of experiments were programmed whose concentration of *p*-HBZH was varied, keeping constant pH, ionic strength, and temperature. The dependence of v_0 with the substrate concentration shown in Fig. 1. It can be observed that for all concentrations of oxidant $[Fe(CN)_6]^{3-}$, the initial reaction rate increases when the *p*-HBZH concentration, [*p*-HBZH], increases, tending to the maximum/constant v_0 corresponding to a zero reaction order.

The best fit of the experimental data was obtained for the rational *Equation (5)*.

$$v_0 = \frac{A[R-BZH]}{B + C[R-BZH]} \quad (5)$$

Table 2 shows the parameters A, B, and C for *p*-HBZH. In principle, these parameters should depend on $[[Fe(CN)_6]^{3-}]$, [Ru(VI)], pH, I and temperature.

The supporting information includes additional figures and tables depicting the influence of the initial reaction rate on the concentration of all substituted aldehydes studied in this work.

3.2. Influence of hexacyanoferrate (III) concentration on the initial reaction rate

To perform this analysis, a series of experiments were carried out where only the $[Fe(CN)_6]^{3-}$ concentration was varied keeping the concentrations of NaOH (0.15 M), Ru(VI) (3.00×10^{-6} M), ionic strength (0.5 M), and temperature (25 °C) constant. The results are shown in Fig. 2.

The mathematical expression that interprets the observed dependence of v_0 on $[Fe(CN)_6]^{3-}$ is given by *equation (6)*.

$$v_0 = \frac{A[[Fe(CN)_6]^{3-}]}{B + C[[Fe(CN)_6]^{3-}]} \quad (6)$$

Parameters A, B, and C should depend on the substrate concentration, [R-BZH], [Ru(VI)], pH, I and temperature. In Fig. 2, it can be seen

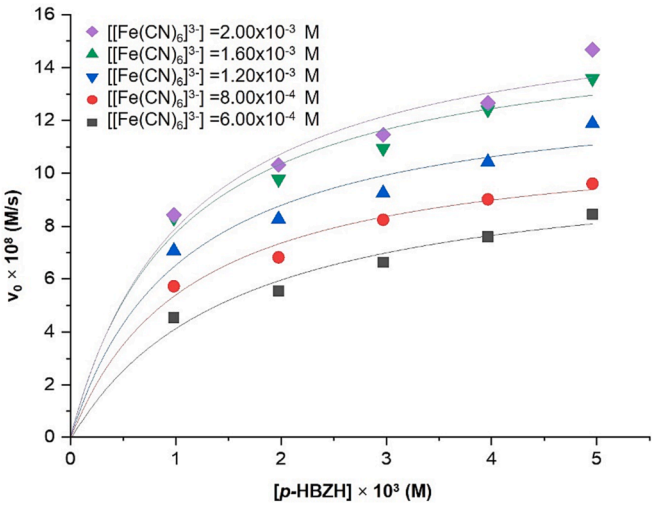

Fig. 1. Influence of substrate concentrations on the initial reaction rate. Experimental conditions: [Ru(VI)] = 3.00×10^{-6}M; I = 0.5 M; T = 25 °C; pH = 12.3.

Table 2
Experimental parameters for the mathematical fit.

$[[Fe(CN)_6]^{3-}] \times 10^3$ M	A (M/s^3)	B $\times 10^{-4}$(M/s^2)	C $\times 10^{-7}$(s^{-2})
0.60	2.15 ± 0.01	3.27 ± 0.02	2.12 ± 0.03
0.80	4.06 ± 0.03	4.14 ± 0.03	3.70 ± 0.03
1.20	9.77 ± 0.02	8.05 ± 0.01	7.66 ± 0.03
1.60	1.75 ± 0.003	1.20 ± 0.02	1.18 ± 0.03
2.00	1.83 ± 0.01	1.27 ± 0.01	1.16 ± 0.03

Experimental conditions: [Ru(VI)] = 3.00×10^{-6}M; I = 0.5 M; T = 25 °C; pH = 12.3.

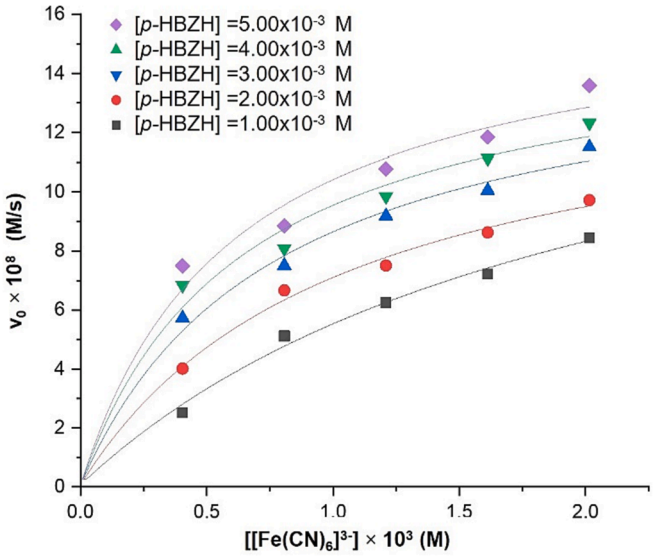

Fig. 2. Influence of hexacyanoferrate concentration on the initial reaction rate. Experimental conditions: [Ru(VI)] = 3.00×10^{-6}M; I = 0.5 M; T = 25 °C; pH = 12.3.

that, for each concentration of *p*-hydroxybenzaldehyde, $[[Fe(CN)_6]^{3-}]$ increases. The initial reaction rate increases until it reaches a constant value. This variation can be fitted to the mathematical expression given by *equation (6)*. The fitting parameters A, B, and C are summarized in Table 3.

The supporting information contains additional figures and tables illustrating the influence of hexacyanoferrate(III) concentration on the initial reaction rate for different substituted aldehydes. The respective parameters A, B, and C are also tabulated in the SI for each R-BZH.

3.3. Influence of Ru (VI) concentration on the initial reaction rate

In this case, a series of experiments were carried out in which the concentration of ruthenate was varied, while the concentrations of R-BZH, $[Fe(CN)_6]^{3-}$, and NaOH were kept constant. In this case, the initial rate in absence of catalyst has not been subtracted. The ionic strength (0.5 M) and temperature were also maintained constant. The experimental data are shown in Table 4 for *p*-HBZH. The stated experimental

Table 3
Experimental reagent concentrations and the fitting parameters to Eq. (6).

[*p*-HBZH] $\times 10^3$ M	A (M/s^3)	B $\times 10^{-4}$(M/s^2)	C $\times 10^{-6}$(s^{-2})
1.00	6.13 ± 0.03	5.13 ± 0.03	4.80 ± 0.03
2.00	5.39 ± 0.01	9.26 ± 0.003	0.01 ± 0.01
3.00	3.25 ± 0.02	4.94 ± 0.02	0.01 ± 0.01
4.00	1.64 ± 0.02	0.77 ± 0.01	0.95 ± 0.02
5.00	3.10 ± 0.3	1.45 ± 0.1	1.51 ± 0.02

Experimental conditions: [Ru(VI)] = 3.00×10^{-6}M; I = 0.5 M; T = 25 °C; pH = 12.3.

Table 4
Influence of Ru(VI) on the initial rate.

[Ru (VI)] × 10^6 (M)	0.75	1.50	3.00	3.75	4.60
$v_0 \times 10^7$ ($M \cdot s^{-1}$)	2.32 ± 0.01	4.57 ± 0.03	7.30 ± 0.02	10.28 ± 0.02	11.40 ± 0.01

Experimental Conditions: [BZH] = 3.00 × 10^{-3} M; [$[Fe(CN)_6]^{3-}$] = 8.00 × 10^{-4}M; I = 0.5 M; T = 25 °C; pH = 12.3.

Table 5
Initial rates obtained at different ionic strengths.

I (M)	1.0	0.8	0.5	0.1
$v_o \times 10^7$ (M/s)	7.89 ± 0.03	7.32 ± 0.01	7.79 ± 0.02	7.40 ± 0.02

Experimental Conditions: [BZH] = 3.00 × 10^{-3} M; [$[Fe(CN)_6]^{3-}$] = 8.00 × 10^{-4}M; [Ru(VI)] = 3.00 × 10^{-6}M; T = 25 °C; pH = 12.3.

uncertainties in v_0 represent the standard deviation of the arithmetic mean from five independent experiments.

A linear relationship between v_0 and the concentration of catalyst was observed for all R-BZH (*Equation (7)*).

$$v_0 = a + b[Ru(VI)] \tag{7}$$

In this example, the y-intercept, *a*, is (2.87 ± 1.89) × 10^{-8} M/s, and the slope, *b*, is (0.266 ± 0.006) s^{-1}. The obtained value for the y-intercept is in excellent agreement with v_0 for the uncatalyzed oxidation reaction. This implies that the reaction order with respect to Ru(VI) is one.

3.4. Influence of the ionic strenght on the initial reaction rate

The effect of ionic strength on the kinetic coefficients depends on the magnitude and sign of the charges of the reactants [17]. No effect of ionic strength on v_0 was observed in this work, "at least" one of the species involved in the rate limiting step is neutral. Table 5 shows the initial rate values obtained at different ionic strength values.

3.5. Solvent isotope effect

In order to determine if the water molecule is involved in the reaction, the isotopic kinetic effect of the solvent has been analyzed using 50 % H_2O/D_2O mixtures [18]. For *p*-HBZH it has been observed that the initial rate in the absence of deuterated water is (7.79 ± 0.02) × 10^{-7} M/s, while in the presence of D_2O v_{0D} was (8.10 ± 0.05) × 10^{-7} M/s. The v_0/v_{0D} ratio of 0.95, which indicates that the water molecule does not influence in the oxidation reaction of R-BZH.

3.6. Products determination

The oxidation products were identified using ^{1}H NMR in 25 experiments carried out under kinetic conditions: [BZH] = 3.00 × 10^{-3} M, [$[Fe(CN)_6]^{3-}$] = 1.20 × 10^{-3} M, I = 0.5 M, pH = 12.3, at 25 °C. The reaction was stopped after 15 min, acidulated, and the organic products were extracted with diethyl ether. The organic phase was dried with magnesium sulfate, filtered, and then the solvent was evaporated. In addition to benzaldehyde, the presence of benzoic acid was detected as reaction product. The comparison of the ^{1}H NMR spectrum obtained from the liquid fraction vs. the ^{1}H NMR spectrum of benzoic acid and benzaldehyde are presented in the supporting information.

4. Discussion

To justify all the experimental results, a reaction mechanism is proposed where the acid-base equilibria of the catalyst *(8)* and *(9)* were considered.

Table 6
Percentages for each aldehydic hydration stage.

Compounds	R-BZH	HydR-BZH	HydR-BZH^-
p-NBZH	27.76	4.72	67.52
BZH	97.11	1.07	1.83
p-MoxBZH	99.23	0.61	0.16
p-HBZH	99.50	0.48	0.02

$$[RuO_4]^{2-} + OH^- \overset{K_1}{\rightleftharpoons} [RuO_4(OH)]^{3-} \tag{8}$$

$$[RuO_4(OH)]^{3-} + OH^- \overset{K_2}{\rightleftharpoons} [RuO_4(OH)_2]^{4-} \tag{9}$$

In order to obtain the experimental reaction rate, the active catalyst species must be $[RuO_4]^{2-}$ and $[RuO_4(OH)]^{3-}$. Moreover, the hydration equilibria of the substrate R-BZH, (*reactions (10) and (11)*) has to be considered. In basic medium, the ionic hydrated species can be oxidized via *equilibrium (11)*.

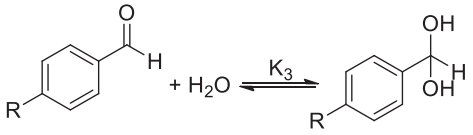

(10)

(R-BZH) *(HydR-BZH)*

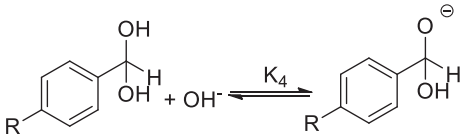

(11)

(HydR-BZH) *(HydR-BZH⁻)*

Taking into account our experimental conditions and the equilibrium constants given by McClelland et al. [19,20], the distribution of the different species in the reaction mixture can be evaluated. The values of K_3 and K_4 for each benzaldehyde derivative can be found in the supporting information. As shown in Table 6, all studied benzaldehydes are present in their carbonyl form except for *p*-nitrobenzaldehyde (*p*-NBZH), which is in its anionic hydrated form.

The first active species of the catalyst, $[RuO_4]^{2-}$, forms the activated complex $[C_1]^{3-}$ through *reaction (12)*. This complex decomposes producing the reduced catalyst species $[RuO_3(OH)]^{3-}$ and the corresponding carboxylic acid.

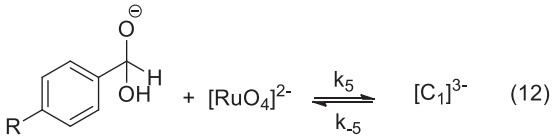

(12)

(HydR-BZH⁻)

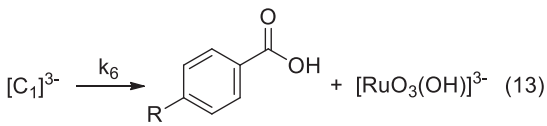

(13)

(P)

Moreover, the second active species of the catalyst, $[RuO_3(OH)]^{3-}$, regenerates $[RuO_4]^{2-}$ by reaction with hexacyanoferrate(III) through *reactions (14)–(16)* [21].

$$[RuO_3(OH)]^{3-} + [Fe(CN)_6]^{3-} \overset{k_7}{\rightarrow} [RuO_3(OH)]^{2-} + [Fe(CN)_6]^{4-} \tag{14}$$

$$[RuO_3(OH)]^{2-} + [Fe(CN)_6]^{3-} \rightarrow [RuO_3(OH)]^{-} + [Fe(CN)_6]^{4-} \tag{15}$$

$$[RuO_3(OH)]^- + OH^- \rightarrow [RuO_4]^{2-} + H_2O \quad (16)$$

The same reaction scheme is applicable to $[RuO_3(OH)]^{3-}$ which forms the activated complex $[C_2]^{4-}$ (see scheme 1). Scheme 1 depicts both catalytic cycles and a proposal for the structure of the activated complexes $[C_1]^{3-}$ and $[C_2]^{4-}$. For simplicity, both catalytic forms are assumed to have the same reactivity. Therefore, the rate constant k_5 will be equal to k_8 and successively (see on the supporting information) [22]. This simplification has been made using Hammond's postulate, which states that two species with similar energies during the course of a reaction will have the same structure and similar reactivities [23,24].

Based on the proposed mechanism, the rate equation for the disappearance of hexacyanoferrate(III) can be expressed according to *equation (17)*.

$$\frac{-d[[Fe(CN)_6]^{3-}]}{dt} = 2k_7[[RuO_3(OH)]^{3-}][[Fe(CN)_6]^{3-}] + 2k_7[[RuO_3(OH)_2]^{4-}][[Fe(CN)_6]^{3-}] \quad (17)$$

At a fixed concentration of hydroxyl ions and at constant temperature, *equation (17)* can be rewritten as a function of the first active catalyst species as shown in *equation (18)*. In the supplementary material, the complete deduction of the rate equation can be found.

$$\frac{-d[\left[Fe(CN)_6\right]^{3-}]}{dt} = \frac{2k_5k_6k_7K_A\left[[Fe(CN)_6]^{3-}\right][R-BZH]_0[Ru(VI)]_0}{k_5k_6K_A[R-BZH]_0 + k_7(k_{-5} + k_6)K_BK_C[[Fe(CN)_6]^{3-}] + k_5k_7K_A\left[[Fe(CN)_6]^{3-}\right][R-BZH]_0} \quad (18)$$

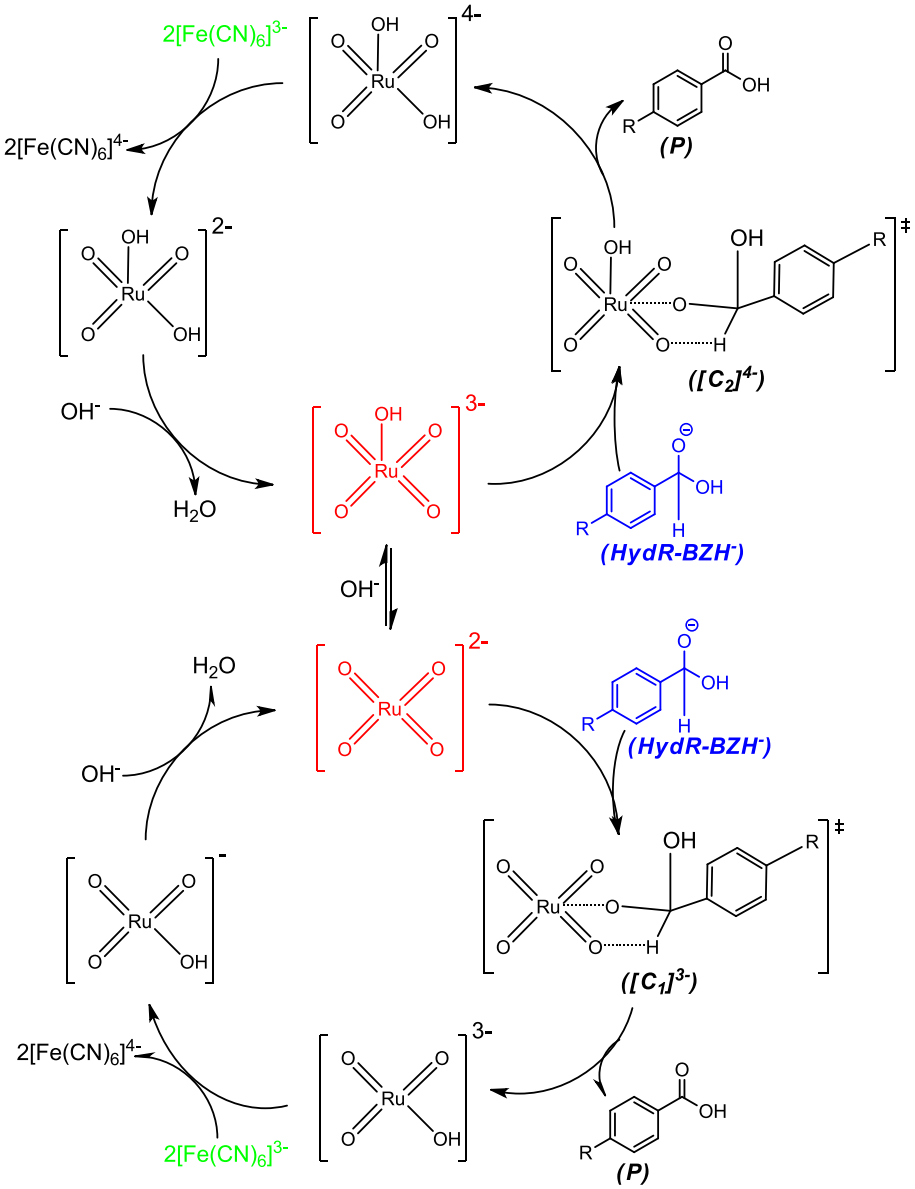

Scheme 1. Catalytic Cycle.

Table 7
Obtained rate constant k_6 for the investigated aldehydes and the σ parameter.

Aldehyde	k_6 (s^{-1})	σ [26]
p-NBZH	2.21 ± 0.03	0.78
BZH	0.85 ± 0.01	0.00
p-MoxBZH	(8.06 ± 0.02) × 10^{-2}	−0.27
p-HBZH	(9.73 ± 0.01) × 10^{-3}	−0.92

Experimental conditions: [Ru(VI)] = 3.00 × 10^{-6}M; I = 0.5 M; T = 25 °C; pH = 12.3.

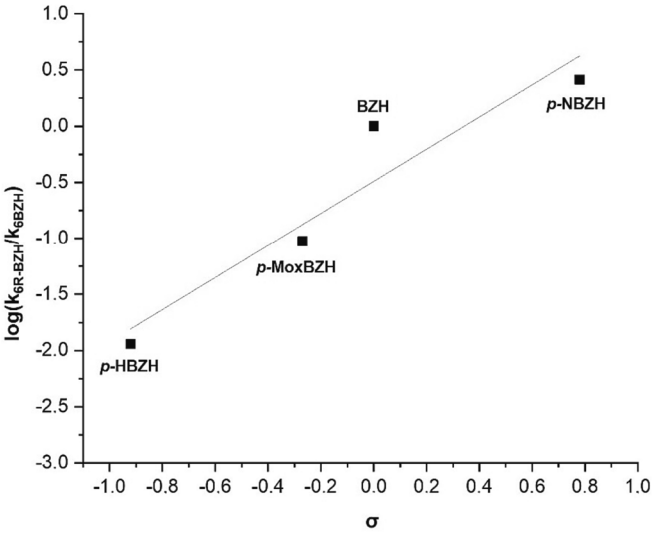

Fig. 3. Plot of Hammett equation for k_6 from Table 7.

Where K_A, K_B and K_C are given by Eqs. (19)–(21), respectively.

$$K_A = K_1[OH^-] + 1 \tag{19}$$

$$K_B = K_1K_2[OH^-]^2 + K_1[OH^-] + 1 \tag{20}$$

$$K_C = 1 + K_3 + K_3K_4[OH^-] \tag{21}$$

Therefore, this theoretical rate *equation (18)* justifies the experimental results of this work where it has been observed that the reaction order with respect to the catalyst, in this case Ru(VI) is one, while the reaction order with respect to $[Fe(CN)_6]^{3-}$ and the substrate changes from one to zero.

Taking into account, the proposed mechanism as well as the obtained results, the rate constant k_6, which is related to the decomposition of complex $[C_1]^{3-}$, was determined for each aldehyde (see Table 7). To analyze the influence of the substituents on k_6, the reactivity-structure correlation was analyzed using Hammett *equation* (22) [25].

$$\log\left(\frac{k_{R-BZH}}{k_{BZH}}\right) = \sigma\rho \tag{22}$$

Table 7 shows the complex decomposition constant, k_6, together with the Hammett parameter σ [26]. In this table, it can be observed that k_6 decreases as σ decreases.

Fig. 3 shows the Hammett plot given by *equation (22)*. *From the* linear regression of the data in Table 7, the obtained Hammett parameter ρ was (1.43 ± 0.01). A positive ρ value implies that the generation of a negative charge or the loss of a positive charge in the activated complex. In other words, benzaldehyde derivatives with electron-donating substituents react more slowly than the parent benzaldehyde and much slower than those with electron-withdrawing substituents.

5. Conclusions

To deepen in the knowledge of the oxidation mechanisms, a comprehensive kinetic study was conducted, focusing on the reactions that involve hexacyanoferrate (III) as economical cooxidant, Ru(VI) as catalyst, and benzaldehyde derivatives as organic substrates. This Ru (VI)-catalyzed process has never been described in bibliography.

In this work, a non-linear relationship between the reaction rate and the concentration of the oxidant and substrate was found implying a complex partial reaction order. These orders change from one to zero reaching a maximum constant initial rate. In contrast, the reaction order with respect Ru(VI) is one. Radhakrishnamurti et al., who used Ru(III) as catalyst, concluded that the reaction order with respect to the substrate was also complex, however with respect to hexacyanoferrate(III) was one [27]. A comparison of reaction rate values for the same experimental conditions reveals that the values obtained in this work are higher, indicating that Ru(IV) serves as a more efficient oxidant than Ru (III). Furthermore, Ru(III) is a one-electron oxidant [28] which leads to the appearance of free radicals and therefore a greater amount of unwanted reaction byproducts. This fact does not occur in the case of Ru (VI), making it a better catalyst.

The proposed mechanism for the Ru(VI)-catalyzed reaction of benzaldehyde derivatives involves the formation of two activated complexes between the anionic hydrated substrate species and the active species of the catalyst. These complexes decompose to form benzoic acid and Ru(IV). The formed Ru(IV) regenerates the active Ru (VI) species. The role of hexacyanoferrate (III) is the regeneration of the catalyst. The theoretical equation obtained from the reaction mechanism, closely match the experimental rate equation, providing strong evidence for the validity of the proposed mechanism.

The positive value of the Hammett parameter ρ implies that the presence of electron-donating substituents in benzaldehyde derivatives leads to slower reaction rates compared to benzaldehyde and those with electron-withdrawing substituents. Thus, when deactivating groups are placed in para position the decomposition of the complexes increases, and the yield in benzoic acid increases too.

This study holds great significance in organic chemistry, particularly for benzaldehyde derivatives, benzoic acid and their industrial applications. The combination of Ru(VI) catalyst and hexacyanoferrate(III) as a cooxidant provide economic and environmental advantages, making it an attractive option for various industries. On the other hand, must be considered that Ru(VI) is very selective because it only oxidizes certain organic bonds.

The knowledge of kinetics and mechanism in this oxidation process opens new possibilities for developing more efficient and eco-friendly oxidation methods, with potential implications in pharmaceuticals, chemicals, and other fields that rely on oxidation reactions.

Funding

Financial support from the University of Castilla-La Mancha and the European Regional Development Fund (FEDER) (grant n° 2023-GRIN-34143) is gratefully acknowledged.

CRediT authorship contribution statement

C.I. Alcolado: Formal analysis, Data curation, Investigation, Writing – original draft, Writing – review & editing. **J. Poblete:** Formal analysis, Investigation. **L. García-Río:** Conceptualization, Formal analysis, Writing – review & editing. **E. Jiménez:** Funding acquisition, Project administration, Writing – review & editing. **F.J. Poblete:** Conceptualization, Formal analysis, Methodology, Supervision, Data curation, Investigation, Writing – original draft, Writing – review & editing.

Declaration of Competing Interest

The authors declare that they have no known competing financial interests or personal relationships that could have appeared to influence the work reported in this paper.

Data availability

I have shared the link to my data at the attach file step

Acknowledgements

Authors acknowledge Juan Tejada Sojo, Dept. of Inorganic, Organic Chemistry and Biochemistry, Faculty of Chemical Science and Technologies, University of Castilla-La Mancha (UCLM), Spain, for providing the ^{1}H-RMN facility for analysis and interpretation.

Appendix A. Supplementary material

Supplementary data to this article can be found online at https://doi.org/10.1016/j.molliq.2023.123580.

References

[1] A. Andersen, Final report on the safety assessment of benzaldehyde, Toxicol. Int. J. 25 (1) (2006) 11–27, https://doi.org/10.1080/10915810600716612.
[2] H. Fujita, T. Fukuju, T. Matsuda, T. Hata, Y. Nishiuchi, M. Sakamoto, Oxidation of benzaldehyde to benzoic acid using O2 fine bubbles, J. Jpn. Pet. Inst. 64 (1) (2021) 10–16, https://doi.org/10.1627/jpi.64.10.
[3] A. Bera, B. Pal, K.K.S. Gupta, Outer-sphere reduction of hexacyanoferrate (III) by enolizable and nonenolizable aldehydes in alkaline medium, Int. J. Chem. Kinet. 44 (7) (2012) 494–505, https://doi.org/10.1002/kin.20616.
[4] C.I. Alcolado, L. García-Río, J.C. Mejuto, I. Moreno, F.J. Poblete, J. Tejeda, Oxidation of aldehydes used as food additives by peroxynitrite, Antioxidants 12 (3) (2023) 743, https://doi.org/10.3390/antiox12030743.
[5] S. Dey, G.C. Dhal, Applications of rhodium and ruthenium catalysts for CO oxidation: an overview, Polytechnica 3 (2020) 26–42, https://doi.org/10.1007/s41050-020-00023-5.
[6] M. Schröder, W.P. Griffith, Potassium ruthenate: a catalytic oxidant for organic subtrates, Omm. J. Chem. Soc. Chem. (1979) 58, https://doi.org/10.1039/C39790000058.
[7] T.V. Lalitha, B. Sethuram, Ruthenium(VI) in the oxidation of 2-propanol and 1-propanol: A kinetic study, Chem. Trans. Met. 17 (1) (1992) 29–33, https://doi.org/10.1007/BF03325411.
[8] P.A. Carson, Hazardous Chemicals Handbook, 2nd ed., Butterworth-Heinemann, Oxford, Wobum, 2002.
[9] K.S. Egorova, V.P. Ananikov, Toxicity of metal compounds: knowledge and myths, Organometallics 36 (21) (2017) 4071–4090, https://doi.org/10.1021/acs.organomet.7b00605.
[10] P.H. Dixneuf, C. Bruneau, Ruthenium in catalysis, Springer, 2014.
[11] S. Rup, F. Zimmermann, E. Meux, M. Schneider, M. Sindt, N. Oget, The ultrasound-assisted oxidative scission of monoenic fatty acids by ruthenium tetroxide catalysis: Influence of the mixture of solvents, Ultrason. Sonochem. 16 (2) (2008) 266–272, https://doi.org/10.1016/j.ultsonch.2008.08.003.
[12] A. Carrington, M.C.R. Symons, Structure and reactivity of the oxyanions of transition metals. Part VII. Kinetics and mechanism of the alkaline decomposition of per-ruthenate, Soc. J. Chem. (1960) 284, https://doi.org/10.1039/JR9600000284.
[13] R.P. Larsen, L.E. Ross, Spectrophotometric determination of ruthenium, Chem. Anal. 31 (2) (1959) 176–178, https://doi.org/10.1021/ac60146a004.
[14] D.G. Lee, The oxidation of tetrahydrofuran by Ruthenium tetraoxide, Chem. Can. J. 50 (1972) 2000, https://doi.org/10.1139/v72-501.
[15] R.E. Connick, C.R. Hurley, Chemistry of Ru(VI), (VII) and –(VIII). reactions, oxidation potentials and spectra, Soc J Am. Chem. 74 (1952) 5012, https://doi.org/10.1021/ja01140a007.
[16] S.L. Fernandez, Técnicas de ajuste de las curvas de concentración en cinética química Retrieved from Tendencias, En Docencia e Investigación En Química 1 (1) (2016) 323–329. http://hdl.handle.net/11191/5146.
[17] K.J. Laidler, Chemical Kinetics, 3rd ed., Pearson India, 2003.
[18] J. Albery, *Solvent Isotope Effects.* in: Caldin, E., Gold, V. (eds) Springer, Boston, MA, 1975, doi: 10.1007/978-1-4899-3013-2_9.
[19] R.A. McClelland, M. Coe, Structure-reactivity effects in the hydration of benzaldehydes, J. Am. Chem. Soc. 105 (9) (1983) 2718–2725, https://doi.org/10.1021/ja00347a033.
[20] R.P. Bell, P.E. Sørensen, Kinetics of the addition of hydroxide ions to substituted benzaldehydes. J. Chem. Soc. Perkin Trans. 2 (13) (1976) 1594–1598, https://doi.org/10.1039/P29760001594.
[21] E.C. Cayuela, L. García-Río, I. Moreno, F.J. Poblete, Quantitative structure-activity relationships in alcohols oxidation using Ru (III) or Ru (VI), J. Mol. Liq. 283 (1) (2019) 843–848, https://doi.org/10.1016/j.molliq.2019.03.114.
[22] D. Fărcaşiu, The use and misuse of the Hammond postulate, J. Chem. Educ. 52 (2) (1975) 76, https://doi.org/10.1021/ed052p76.
[23] F.J. Poblete, P. Corrochano, Alcohol Oxidation catalysed by Ru(VI) in the presence of alkaline hexacyanoferrate(III), Chem. J. Phys. Org 23 (11) (2010) 1088–1092, https://doi.org/10.1002/poc.1780.
[24] F.A. Carey, R.J. Sundberg, Advanced Organic Chemistry.-Part A: Structure and Mechanism, Plenum, Berlin New York, NY, 1999.
[25] L.P. Hammett, The effect of structure upon the reactions of organic compounds. Benzene Derivatives, J. Am. Chem. Soc. 59 (1937) 96–103, https://doi.org/10.1021/ja01280a022.
[26] C.D. Ritchie, W.F. Sager, An examination of structure-reactivity relationships, Prog. Phys. Org. Chem. 2 (1964) 323–400, https://doi.org/10.1002/9780470171813.ch6.
[27] P.S. Radhakrishnamurti, B.R.K. Swamy, Kinetics of ruthenium(III)-catalysed oxidation of aromatic aldehydes by alkaline ferricyanide, Proc. Indian Acad. Sci. (chem.sci.) 88 (3) (1979) 163–170, https://doi.org/10.1007/BF02844797.
[28] A.E. Mucientes, R.E. Gabaldón, F.J. Poblete, S. Villarreal, Comparative study of the catalytic behaviour of Ru (III) and Ru (VI) on the oxidation of alcohols by hexacyanoferrate (III), J. Phys. Org. Chem. 17 (3) (2004) 236–240, https://doi.org/10.1002/poc.721.